Journal of Microbiology (2014) Vol. 52, No. 7, pp. 619–625
DOI 10.1007/s12275-014-3479-4

Bovine Viral Diarrhea Virus Infection Induces Autophagy in MDBK Cells

Qiang Fu[1†], Huijun Shi[1†], Yan Ren[2], Fei Guo[2], Wei Ni[3], Jun Qiao[1], Pengyan Wang[1], Hui Zhang[1], and Chuangfu Chen[1*]

[1]College of Animal Science and Technology, [2]College of Medicine, [3]College of Life Science, Shihezi University, Shihezi 832003, Xinjiang, P.R. China

(Received Sep 13, 2013 / Revised Feb 20, 2014 / Accepted Apr 5, 2014)

Bovine viral diarrhea virus (BVDV) is an enveloped, positive-sense, single-stranded RNA virus that belongs to the genus *Pestivirus* (Flaviviridae). The signaling pathways and levels of signaling molecules are altered in Madin-Darby Bovine Kidney (MDBK) cells infected with BVDV. Autophagy is a conservative biological degradation pathway that mainly eliminates and degrades damaged or superfluous organelles and macromolecular complexes for intracellular recycling in eukaryotic cells. Autophagy can also be induced as an effective response to maintain cellular homeostasis in response to different stresses, such as nutrient or growth factor deprivation, hypoxia, reactive oxygen species exposure and pathogen infection. However, the effects of BVDV infection on autophagy in MDBK cells remain unclear. Therefore, we performed an analysis of autophagic activity after BVDV NADL infection using real-time PCR, electron microscopy, laser confocal microscopy, and Western blotting analysis. The results demonstrated that BVDV NADL infection increased autophagic activity and significantly elevated the expression levels of the autophagy-related genes Beclin1 and ATG14 in MDBK cells. However, the knockdown of Beclin1 and ATG14 by RNA interference (RNAi) did not affect BVDV NADL infection-related autophagic activity. These findings provided a novel perspective to elaborate the effects of viral infection on the host cells.

***Keywords*:** bovine viral diarrhea virus NADL, autophagy, Madin-Darby Bovine Kidney (MDBK) cells, autophagosome, GFP-LC3

Introduction

Bovine viral diarrhea virus (BVDV) is a major cause of economic losses to the cattle industry and distributed throughout the world (Perdrizet *et al*., 1987). BVDV belongs to the genus *Pestivirus* in the family Flaviviridae which also includes classical swine fever virus and border disease virus (Hulst *et al*., 2000). Based on differences in the 5′ untranslated region (UTR) of the BVDV genome, BVDV isolates are divided into genotypes I and II (Ridpath *et al*., 1994). BVDV isolates can also be divided into non-cell pathogenic (ncp) and cell pathogenic (cp) types based on the observed cytopathic effects (CPEs) in target cell culture (Mendez *et al*., 1998).

Autophagy is a quality control system by which the cell degrades components or organelles in the cytoplasm in response to nutrient deficiency, certain cytotoxins, and endoplasmic reticulum (ER) stress, thereby ultimately removing damaged or surplus organelles and macromolecular complexes (Klionsky, 2007; Mizushima, 2007). More than 30 autophagy-related genes (ATGs) are involved in the regulation mechanisms and signaling pathways of autophagy in mammalian cells (He and Klionsky, 2009; Mehrpour *et al*., 2010). Among these ATGs, Beclin1 (Kang *et al*., 2011) and ATG14 (Obara and Ohsumi, 2011) form a complex that is involved in autophagy. With regard to the methods utilized to monitor monitoring autophagy, the most common method is electron microscopy (Ashford and Porter, 1962). The autophagic double-membrane structure, the autophagosome, was discovered by electron microscopy (Klionsky *et al*., 2012). In addition, some biochemical methods have been employed to measure autophagic activity. Microtubule-associated protein 1A/1B-light chain 3 (LC3), a reliable marker of autophagosomes in eukaryotic cells, is required for autophagosome formation (Kadowaki and Karim, 2009). During autophagy, the protein LC3 is recruited to the autophagosomal membrane (Klionsky *et al*., 2012), and a cytosolic form of LC3 (LC3-I; approximately 16 kDa) is conjugated to phosphatidylethanolamine to form the LC3-phosphatidylethanolamine conjugate (LC3-II; approximately 14 kDa) (Tanida *et al*., 2008).

Complex interactions between pathogens and the autophagic process have recently been reported. The unfolded protein response (UPR), which is induced by hepatitis C virus (HCV), activates autophagy to favor the virus life cycle (Ke and Chen, 2011a). Moreover, dengue virus (DENV) infection activates the autophagic pathway-dependent processing of lipid droplets and triglycerides to release free fatty acids, which are required for efficient DENV replication (Heaton and Randall, 2010). Research has also shown that coxsackievirus B3 (CVB3) infection triggers autophagosome formation and that inhibition of the autophagosome significantly reduces CVB3 replication (Wong *et al*., 2008). Autophagy is a common event in varicella-zoster virus (VZV)-infected cells and is provoked at least, in part, by ER stress secondary to overly abundant VZV glycoprotein biosyn-

†These authors contributed equally to this work.
*For correspondence. E-mail: cfchen1964@gmail.com; Tel.: +86-993-2058002; Fax: +86-993-2058612

thesis, which leads to UPR activation in an attempt to maintain cellular homeostasis (Carpenter *et al.*, 2011). Although numerous studies have clarified the interactions between various viruses and autophagy, the effects of BVDV infection on autophagic activity have not been investigated to date. This information is necessary for a full understanding of BVDV and would be helpful in elucidating BVDV pathogenesis and the host cellular responses to BVDV infection.

In this study, we analyzed autophagosome formation, the percentage of autophagic cells and the expression levels of the autophagy-related genes, Beclin1 and ATG14. The results showed that autophagy was significantly induced due to BVDV infection in MDBK cells and that the expression levels of Beclin1 and ATG14 were also significantly increased. Of interest, the downregulation of Beclin1 and ATG14 by RNAi did not affect BVDV NADL-induced autophagy.

Materials and Methods

Cell culture and virus

The MDBK cell line was purchased from the Cell Bank of Type Culture Collection of the Chinese Academy of Sciences (China) and maintained in Roswell Park Memorial Institute (RPMI) 1640 medium supplemented with 10% heat-inactivated horse serum, 1% non-essential amino acids (NEAA) in Modified Eagle's Medium (MEM), 2 mM L-glutamine, 100 U/ml penicillin, and 0.10 mg/ml streptomycin. All cell culture media and nutritional supplements were obtained from Thermo Fisher Scientific (USA). The MDBK cells and cell culture media were pre-tested and confirmed to be free of BVDV and anti-BVDV antibodies.

The BVDV NADL reference strain (genotype 1a and cp type) (Mendez *et al.*, 1998) was obtained from the National Institutes for Food and Drug Control (China). The viruses were amplified in MDBK cells for 48–72 h. Prior to infection with BVDV NADL, titration of the 50% tissue culture infective dose ($TCID_{50}$) was performed using the Reed and Müench method (Reed and Muench, 1938).

Treatments

The GFP-LC3 plasmid, which was kindly provided by Fei Guo (Guo *et al.*, 2012), was prepared using EndoFree Maxi Plasmid Kit (Tiangen, China) and electroporated into MDBK cells (60 to 70% confluent) with the Bio-Rad Gene Pulser Xcell (Cytomix electroporation buffer, 340 V, 5 ms, 4-mm cuvettes, and one pulse). At 24 h post-transfection, the cells were incubated with 1/10,000 dimethyl sulfoxide (DMSO; negative control) (Sigma, USA), 100 nM rapamycin (autophagy promoter; positive control) (Sigma), or BVDV NADL (100 $TCID_{50}$/ 0.1 ml) at 37°C with 5% CO_2 for 4 h in 6-well plates. The cell supernatants were then discarded and replaced with fresh culture medium, and this point was designated as time point zero after treatments.

Transmission electron microscopy

At 12 h after treatment, the cells treated with DMSO and BVDV NADL were harvested and washed with 0.01 M phosphate-buffered saline (PBS; pH 7.4), followed by fixation with ice-cold glutaraldehyde (4% in PBS; pH 7.4) at 4°C for 30 min. After washing with PBS, the cells were post-fixed in osmium tetroxide (Sigma). The procedures of sample embedding, ultrathin sectioning, and staining with uranyl acetate/lead citrate were performed as previously described (Li *et al.*, 2008). Transmission electronic microscopy (TEM) images were taken on a JEM1230 electron microscope (JEOL Ltd, Japan).

Fluorescence microscopy and laser confocal microscopy

A fluorescence microscope (TE2000; Nikon, Japan) was employed to quantitate the average number of GFP-LC3 puncta-positive cells in ten randomly selected non-overlapping fields per treatment. The percentage of autophagic cells was calculated as follows: percentage of autophagic cells (%) = (a / b) × 100%; where a is the number of autophagic cells; and b is the number of total cells in ten randomly selected fields. The cells were also separately incubated with 1/20,000 (v/v) LysoTracker Red (Beyotime, China) for 1 h. After washing with PBS and fixation with 4% paraformaldehyde, a laser scanning confocal microscope (E600; Riken, Japan) was employed to observe autolysosome formation.

RNA extraction and real-time PCR

The cells were treated with BVDV NADL, rapamycin, or DMSO for various time periods, and total RNA was extracted using the Total RNA Extraction Kit (Tiangen). First-strand cDNA was synthesized from 2 μg of total RNA using a Reverse Transcription Kit (Tiangen). The synthesized cDNA was used immediately for quantitative real-time PCR to analyze the mRNA levels of Beclin1 and ATG14 using a LightCycler 480 (Roche, USA). Data were analyzed by the $2^{-\Delta\Delta Ct}$ Method (Livak and Schmittgen, 2001) and normalized to the endogenous levels of glyceraldehyde 3-phosphate dehydrogenase (GAPDH). The primers for *Bos taurus* Beclin1 (GenBank accession number NM_001033627; forward, 5′-TCCATTACTTGCCACAGCC-3′; reverse, 5′-GCCATCAGATGCCTCCC-3′), ATG14 (GenBank accession number NM_001192099; forward, 5′-CCAGAGCGGCGATTTCGTCTACT-3′; reverse, 5′-CCAAGTTTGCGATTATGCCTCTG-3′), and GAPDH (GenBank accession number NM_001034034; forward, 5′-GGCAAGTTCAACGG CACAG-3′; reverse, 5′-TTCACGCCCATCACAAACA-3′) were designed using Primer Premier 5.0 software (Primer, Canada).

Western blotting analysis

To further detect the protein levels of Beclin1 and ATG14 at different time intervals, approximately 10^6 cells from each treatment were collected and lysed with Cell Lysis Buffer (Beyotime, China). The protein concentration was determined using the BCA Protein Quantification Assay Kit (Tiangen). Equal amounts of protein were subjected to 15% sodium dodecyl sulfate-polyacrylamide gel electrophoresis (SDS-PAGE) and electrophoretically transferred onto a 0.45-μm NitroBind nitrocellulose membrane (Micron Separations, Inc., USA) using the semi-dry electrophoretic transfer method at 200 mA for 1 h. After blocking with PBS containing 5% non-fat milk and 0.1% Tween 20, the membranes were incubated with a rabbit anti-Beclin 1 (Bioworld,

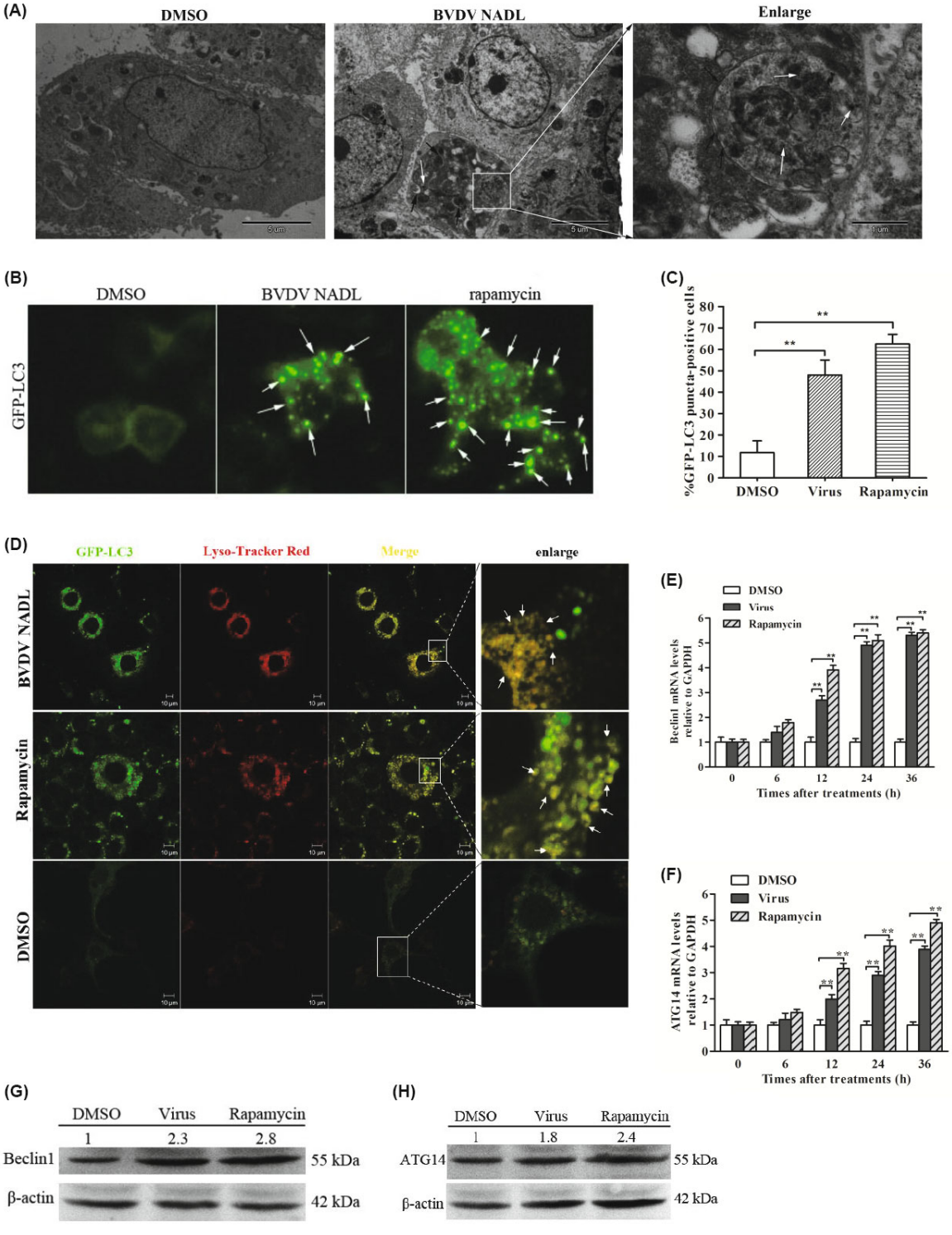

Fig. 1. BVDV NADL infection triggers autophagosome formation and increases autophagic activities. (A) Autophagic double-membrane vesicles (black arrows) enwrapping BVDV NADL viral particles (white arrows) were observed under a transmission electron microscope. (B) MDBK cells transfected with the GFP-LC3 plasmid previously were subsequently treated with BVDV NADL, rapamycin, or DMSO. Numerous GFP-LC3 puncta (white arrows) were observed in cells treated with BVDV NADL and rapamycin. n = 3. (C) Ten fields were randomly selected to determine the percentage of autophagic cells at 12 h after different treatments. The results are shown as the mean ± SD (error bars), n = 3, $^{**}P<0.01$. (D) Laser confocal microscopy imaging showed that an autophagosome was marked with GFP-LC3 dots, co-localized with a red fluorescence-tagged lysosome to the MDBK cell cytoplasm and formed an autolysosome (white arrows) at 12 h after BVDV infection and rapamycin treatment. n = 3. (E) and (F) mRNA levels of Beclin1 and ATG14 were determined at various time intervals by real-time PCR and normalized to GAPDH. The results are shown as the mean ± SD (error bars), n = 3, $^{**}P<0.01$. (G) and (H) Immunoblot analysis showing Beclin1 and ATG14 protein levels following the indicated treatments (n = 2).

MB0030) or ATG14 (Proteintech, 19491-1-AP) antibody, followed by incubation with a goat anti-rabbit IgG (H+L) antibody (Bioworld, BS10350) labeled with horseradish peroxidase (HRP). A rabbit anti-β-actin antibody (Bioworld, AP0733) was used to detect β-actin as an internal control. Immunoreactivity was visualized using the diaminobenzidine kit (Tiangen). Quantifications of protein bands were performed using ImageJ software (National Institutes of Health, USA).

RNA interference and autophagic activity analysis

Short hairpin RNAs (shRNAs) targeting Beclin1 and ATG14 were designed using the online shRNA sequence designer tool (http://www.clontech.com/CN/Support/Online_Tools) and cloned into the *Bam*HI and *Eco*RI sites of the RNAi-Ready pSIREN-RetroQ-ZsGreen vector (Clontech, USA). The top strands of the shRNAs specific for the target genes were as follows: Beclin1, 5′ gatccAGCTCAGTATCAAAGGGAATTCAAGAGATTCCCTTTGATACTGAGCTTTTTTTg 3′; and ATG14, 5′ gatccGTGAAGAAACTGAATGCAAATTCAAGAGATTTGCATTCAGTTTCTTCATTTTTTg 3′. The empty plasmid and recombinant plasmids were individually prepared and co-transfected with the GFP-LC3 plasmid into monolayer MDBK cells (60–70% confluence). At various time intervals post-transfection, the expression levels of Beclin1 and ATG14 were analyzed using real-time PCR and Western blotting as described above. At 24 h post-transfection, the cells were infected with BVDV NADL (100 $TCID_{50}$/ 0.1 ml). The percentage of autophagic cells was evaluated using fluorescence microscopy and Western blotting at different time intervals after BVDV infection.

MTT assays

MDBK cells were plated into 96-well flat-bottom plates (Corning, USA) at a density of 10^4 cells/ well and incubated at 37°C with 5% CO_2 until the cells grew to approximately 60% confluence. The cells were then incubated with BVDV NADL, rapamycin, or DMSO for 36 h as described above. Cell viability was assessed using the MTT Cell Proliferation Assay Kit (ATCC, USA) according to the manufacturer's protocol. The optical density (OD) was measured at 570 nm (OD_{570}) using a TECAN SUNRISE spectrophotometer (TECAN, Switzerland).

Statistical analyses

Statistical analyses were performed using SPSS 17.0 for Window (SPSS Inc., USA). Values of $^*P<0.05$ and $^{**}P<0.01$ were considered to be significant and highly significant, respectively. The results are shown as the mean ± standard deviation (SD), and error bars represent the SD.

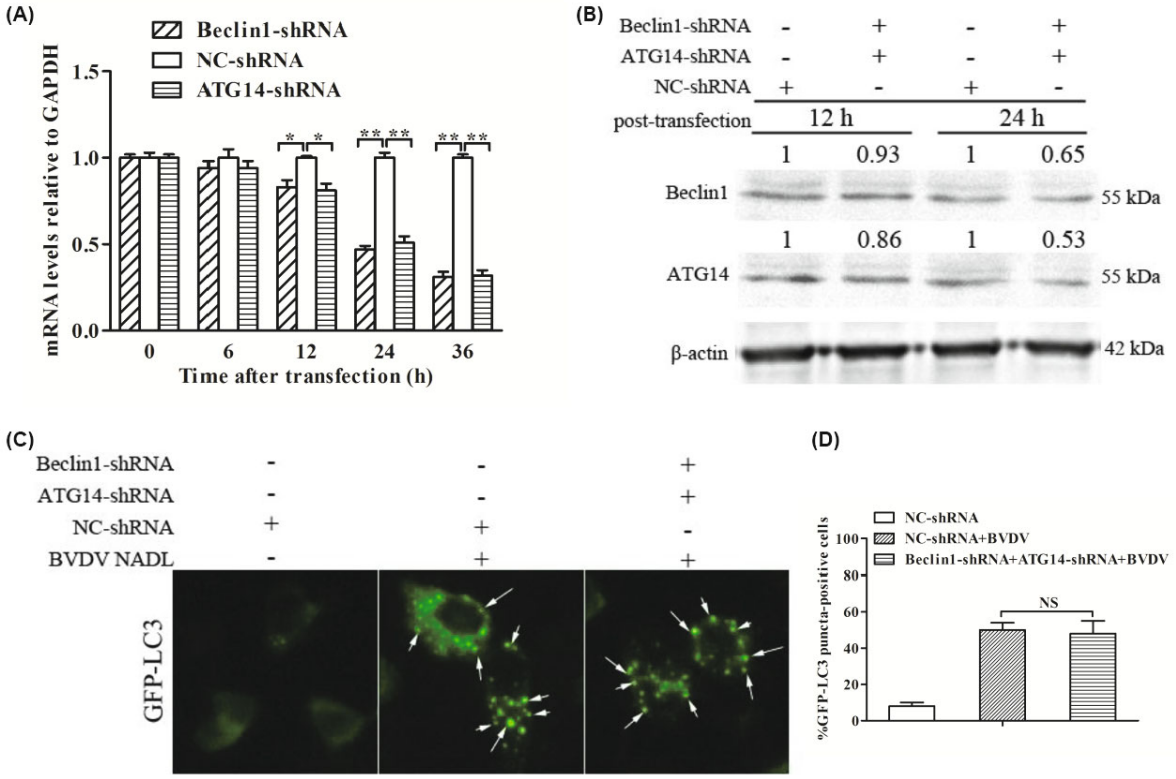

Fig. 2. Beclin1 and ATG14 downregulation does not affect BVDV NADL infection-related autophagy. (A) RNAi was introduced to downregulate Beclin1 and ATG14 expression. Real-time PCR was used to detect the mRNA levels of Beclin1 and ATG14. The results are shown as the mean ± SD (error bars) of three replicate experiments, $^*P<0.05$, $^{**}P<0.01$. (B) Beclin1 and ATG14 protein levels were determined by Western blot analysis (n = 2). (C) and (D) The average number of GFP-LC3 puncta-positive cells were quantitated in ten randomly selected fields, and the percentage of autophagic cells was determined under a fluorescence microscope. The results are shown as the mean ± SD (error bars), n = 3, not significant (NS).

Results

BVDV NADL infection triggered autophagosome and autolysosome formation

Transmission electronic microscopy observations showed that numerous autophagosomes consisting of a double-membrane structure were present in the BVDV-infected MDBK cells with a greater amount in the infected cells than in the DMSO-treated cells (Fig. 1A). To further monitor autophagic activity, the average number of autophagic cells was measured in ten randomly selected fields under a fluorescence microscope (Fig. 1B). The percentage of GFP-LC3 puncta-positive cells was significantly higher in the BVDV NADL- and rapamycin-treated cells than in the negative control cells (Fig. 1C). Using a laser scanning confocal microscope, GFP-LC3 puncta and red fluorescence-tagged lysosomes were co-localized to the MDBK cell cytoplasm after BVDV infection and rapamycin treatment (Fig. 1D).

Beclin1 and ATG14 expression levels were increased as a result of BVDV NADL infection

Beclin1 and ATG14 are crucial autophagy-related genes involved in the process of autophagosome formation. To further confirm autophagic activity, we determined the abundance of Beclin1 and ATG14 using real-time PCR and Western blotting. The results showed that the mRNA and protein levels of Beclin1 and ATG14 were increased in BVDV NADL- and rapamycin-treated cells compared with the DMSO-treated cells (Figs. 1E–H), thereby indicating that autophagic activity was promoted.

The effects of BVDV NADL infection on autophagy were not affected by RNAi targeting Beclin1 and ATG14

To confirm the role of Beclin1 and ATG14 in BVDV NADL-induced autophagy, RNAi sequences targeting Beclin1 and ATG14 were introduced to knockdown the expression levels of these genes. The results showed that the expression levels of Beclin1 and ATG14 were significantly decreased by RNAi (Figs. 2A and 2B). Interestingly, the percentage of autophagic cells (Figs. 2C and 2D) in BVDV NADL-infected MDBK cells was not affected by RNAi.

Neither BVDV infection nor rapamycin treatment affected cell viability

A MTT assay was applied to assess cell viability. The results showed that cell viability was not significantly different among the BVDV NADL-, rapamycin-, and DMSO-treated MDBK cells (Fig. 3), thereby indicating that cell viability was not differently affected by different treatments.

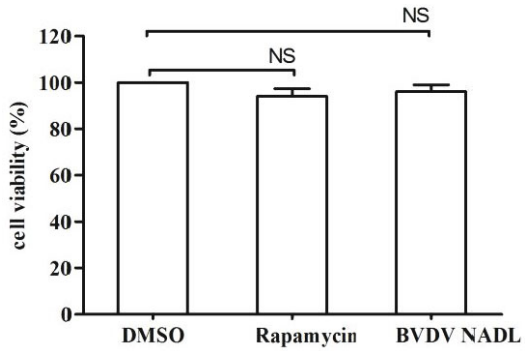

Fig. 3. No significant difference in cell viability was observed among the treated cells. Cell viability was analyzed using the MTT assay after the different treatments. The results are shown as the mean ± SD, n = 3. NS, not significant.

Discussion

Autophagy is recognized as an immune mechanism that is activated when pathogenic microorganisms infect target cells (Deretic, 2006), and it plays a wide variety of physiological and pathophysiological roles in resisting intracellular pathogens (Mizushima *et al.*, 2008; Zhao *et al.*, 2008) as well as in the digestion of dysfunctional intracellular organelles for recycling. Because of the importance of autophagy in maintaining cellular homeostasis, many studies have reported multiple relationships between pathogens and autophagy. For example, enterovirus 71 (Xi *et al.*, 2013) and adenoviruses (Rodriguez-Rocha *et al.*, 2011) induce autophagy in target cells, and autophagy promotes the replication of encephalomyocarditis virus (Zhang *et al.*, 2011) and hepatitis B virus (Li *et al.*, 2011) in host cells. In addition, autophagy also protects against Sindbis virus (SINV) infection of the central nervous system (Orvedahl *et al.*, 2010). In addition to BVDV, viruses in the Flaviviridae family interact with autophagic machinery (Table 1). Regardless, it remains unclear whether BVDV infection induces or affects autophagy in MDBK cells (Dreux and Chisari, 2010).

In our study, we found that autophagy significantly in-

Table 1. The interaction between autophagy and representative strains of Flaviviridae

Flaviviridae		Impact of virus on autophagy	Impact of autophagy on virus replication and viral particles release	References
Genus	Representative strains			
Flavivirus	Dengue virus (DENV)	DENV induces a selective autophagy that stimulates lipid metabolism	Autophagy activated by dengue virus enhances virus replication	Lee *et al.* (2008), Gangodkar *et al.* (2010), Heaton and Randall (2010, 2011), Mateo *et al.* (2013)
Hepacivirus	Hepatitis C virus (HCV)	HCV inhibits AKT-tuberous sclerosis complex (TSC) through ER stress to induce autophagy	The autophagical machinery is required to initiate HCV replication	Dreux *et al.* (2009), Mizui *et al.* (2010), Ke and Chen (2011b), Huang *et al.* (2012), Sir *et al.* (2012)
Pestivirus	Bovine viral diarrhea virus (BVDV)	BVDV NADL infection induces autophagy and increases the expression of Beclin1 and ATG14 in MDBK cells	BVDV genome which was inserted LC3 sequence was apparently a result of genetic recombination	Meyers *et al.* (1998)

creased after BVDV NADL infection in MDBK cells. Autophagosome formation was clearly observed under an electron microscope, and viral particles were engulfed by autophagolysosomes. Numerous GFP-LC3 puncta appeared in the cytoplasm of cells infected with BVDV NADL. To further confirm that BVDV infection significantly increased autophagic activity, we examined the expression levels of autophagy-associated genes. The results showed that the mRNA and protein levels of Beclin1 and ATG14 were significantly upregulated during BVDV NADL infection. Collectively, these findings suggested that autophagy was induced and that its activity increased significantly due to BVDV NADL infection.

Numerous stimuli, such as starvation and oxidative stress, activate the class III PI3 kinase/Beclin1/Atg14 complex to trigger the autophagic process (Ferdous *et al*., 2010). The role of Beclin1 and ATG14 in BVDV NADL-related autophagy was investigated in our study. Of interest, Beclin1 and ATG14 downregulation by RNAi did not affect BVDV NADL infection-induced autophagy. Therefore, we speculate that there are other signaling pathways involved in BVDV infection-induced autophagy, a hypothesis that requires further research.

Although we demonstrated that BVDV infection affected autophagic activity in MDBK cells, our results did not clearly show the effects of autophagy on BVDV replication and viral particle release, and the interactions between autophagy and BVDV infection were not completely clarified. Thus, to further understand the mechanisms by which BVDV infection induces and promotes autophagic activity, we have designed related experiments to investigate the interaction between BVDV NADL and autophagy.

Acknowledgements

We thank Weiwei Cao (College of Medicine, Shihezi University, China) and Hanhua Hu (Xinjiang Medical University, China) for technical assistance with confocal microscopy and electron microscopy, respectively. This work was supported by the International S&T Cooperation Program of China (Grant No. 2013DFR30970) and Natural Science Foundation of China (Grant No. 31101816 and 31360615).

References

Ashford, T.P. and Porter, K.R. 1962. Cytoplasmic components in hepatic cell lysosomes. *J. Cell Biol.* **12**, 198–202.

Carpenter, J.E., Jackson, W., Benetti, L., and Grose, C. 2011. Autophagosome formation during varicella-zoster virus infection following endoplasmic reticulum stress and the unfolded protein response. *J. Virol.* **85**, 9414–9424.

Deretic, V. 2006. Autophagy as an immune defense mechanism. *Curr. Opin. Immunol.* **18**, 375–382.

Dreux, M. and Chisari, F.V. 2010. Viruses and the autophagy machinery. *Cell Cycle* **9**, 1295–1307.

Dreux, M., Gastaminza, P., Wieland, S.F., and Chisari, F.V. 2009. The autophagy machinery is required to initiate hepatitis C virus replication. *Proc. Natl. Acad. Sci. USA* **106**, 14046–14051.

Ferdous, A., Battiprolu, P.K., Ni, Y.G., Rothermel, B.A., and Hill, J.A. 2010. FoxO, autophagy, and cardiac remodeling. *J. Cardiovasc. Transl. Res.* **3**, 355–364.

Gangodkar, S., Jain, P., Dixit, N., Ghosh, K., and Basu, A. 2010. Dengue virus-induced autophagosomes and changes in endomembrane ultrastructure imaged by electron tomography and whole-mount grid-cell culture techniques. *J. Electron Microsc.* **59**, 503–511.

Guo, F., Zhang, H., Chen, C., Hu, S., Wang, Y., Qiao, J., Ren, Y., Zhang, K., Wang, Y., and Du, G. 2012. Autophagy favors *Brucella* melitensis survival in infected macrophages. *Cell Mol. Biol. Lett.* **17**, 249–257.

He, C. and Klionsky, D.J. 2009. Regulation mechanisms and signaling pathways of autophagy. *Annu. Rev. Genet.* **43**, 67–93.

Heaton, N.S. and Randall, G. 2010. Dengue virus-induced autophagy regulates lipid metabolism. *Cell Host Microbe* **8**, 422–432.

Heaton, N.S. and Randall, G. 2011. Dengue virus and autophagy. *Viruses* **3**, 1332–1341.

Huang, H., Kang, R., Wang, J., Luo, G., Yang, W., and Zhao, Z. 2012. Hepatitis C virus inhibits AKT-tuberous sclerosis complex (TSC), the mechanistic target of rapamycin (mTOR) pathway, through endoplasmic reticulum stress to induce autophagy. *Autophagy* **9**, 175–195.

Hulst, M.M., van Gennip, H.G., and Moormann, R.J. 2000. Passage of classical swine fever virus in cultured swine kidney cells selects virus variants that bind to heparan sulfate due to a single amino acid change in envelope protein E^{rns}. *J. Virol.* **74**, 9553–9561.

Kadowaki, M. and Karim, M.R. 2009. Cytosolic LC3 ratio as a quantitative index of macroautophagy. *Methods Enzymol.* **452**, 199–213.

Kang, R., Zeh, H.J., Lotze, M.T., and Tang, D. 2011. The Beclin 1 network regulates autophagy and apoptosis. *Cell Death Differ.* **18**, 571–580.

Ke, P.Y. and Chen, S.S.L. 2011a. Autophagy: a novel guardian of HCV against innate immune response. *Autophagy* **7**, 533–535.

Ke, P.Y. and Chen, S.S.L. 2011b. Activation of the unfolded protein response and autophagy after hepatitis C virus infection suppresses innate antiviral immunity *in vitro*. *J. Clin. Invest.* **121**, 37.

Klionsky, D.J. 2007. Autophagy: from phenomenology to molecular understanding in less than a decade. *Nat. Rev. Mol. Cell Biol.* **8**, 931–937.

Klionsky, D.J., Abdalla, F.C., Abeliovich, H., Abraham, R.T., Acevedo-Arozena, A., Adeli, K., Agholme, L., Agnello, M., Agostinis, P., and Aguirre-Ghiso, J.A. 2012. Guidelines for the use and interpretation of assays for monitoring autophagy. *Autophagy* **8**, 445–544.

Lee, Y.R., Lei, H.Y., Liu, M.T., Wang, J.R., Chen, S.H., Jiang-Shieh, Y.F., Lin, Y.S., Yeh, T.M., Liu, C.C., and Liu, H.S. 2008. Autophagic machinery activated by dengue virus enhances virus replication. *Virology* **374**, 240–248.

Li, M., Jiang, X., Liu, D., Na, Y., Gao, G.F., and Xi, Z. 2008. Autophagy protects lncap cells under androgen deprivation conditions. *Autophagy* **4**, 54–60.

Li, J., Liu, Y., Wang, Z., Liu, K., Wang, Y., Liu, J., Ding, H., and Yuan, Z. 2011. Subversion of cellular autophagy machinery by hepatitis B virus for viral envelopment. *J. Virol.* **85**, 6319–6333.

Livak, K.J. and Schmittgen, T.D. 2001. Analysis of relative gene expression data using real-time quantitative PCR and the $2^{-\Delta\Delta Ct}$ method. *Methods* **25**, 402–408.

Mateo, R., Nagamine, C.M., Spagnolo, J., Méndez, E., Rahe, M., Gale, M., Yuan, J., and Kirkegaard, K. 2013. Inhibition of cellular autophagy deranges dengue virion maturation. *J. Virol.* **87**, 1312–1321.

Mehrpour, M., Esclatine, A., Beau, I., and Codogno, P. 2010. Overview of macroautophagy regulation in mammalian cells. *Cell*

Res. **20**, 748–762.

Mendez, E., Ruggli, N., Collett, M.S., and Rice, C.M. 1998. Infectious bovine viral diarrhea virus (strain NADL) RNA from stable cDNA clones: a cellular insert determines NS3 production and viral cytopathogenicity. *J. Virol.* **72**, 4737–4745.

Meyers, G., Stoll, D., and Gunn, M. 1998. Insertion of a sequence encoding light chain 3 of microtubule-associated proteins 1A and 1B in a pestivirus genome: connection with virus cytopathogenicity and induction of lethal disease in cattle. *J. Virol.* **72**, 4139–4148.

Mizui, T., Yamashina, S., Tanida, I., Takei, Y., Ueno, T., Sakamoto, N., Ikejima, K., Kitamura, T., Enomoto, N., and Sakai, T. 2010. Inhibition of hepatitis C virus replication by chloroquine targeting virus-associated autophagy. *J. Gastroenterol.* **45**, 195–203.

Mizushima, N. 2007. Autophagy: process and function. *Genes Dev.* **21**, 2861–2873.

Mizushima, N., Levine, B., Cuervo, A.M., and Klionsky, D.J. 2008. Autophagy fights disease through cellular self-digestion. *Nature* **451**, 1069–1075.

Obara, K. and Ohsumi, Y. 2011. Atg14: a key player in orchestrating autophagy. *Int. J. Cell Biol.* **2011**, 713435.

Orvedahl, A., MacPherson, S., Sumpter, R., Jr., Talloczy, Z., Zou, Z., and Levine, B. 2010. Autophagy protects against Sindbis virus infection of the central nervous system. *Cell Host Microbe* **7**, 115–127.

Perdrizet, J.A., Rebhun, W.C., Dubovi, E.J., and Donis, R.O. 1987. Bovine virus diarrhea-clinical syndromes in dairy herds. *Cornell. Vet.* **77**, 46–74.

Reed, L.J. and Muench, H. 1938. A simple method of estimating fifty percent endpoints. *Am. J. Epidemiol.* **27**, 493–497.

Ridpath, J.F., Bolin, S.R., and Dubovi, E.J. 1994. Segregation of bovine viral diarrhea virus into genotypes. *Virology* **205**, 66–74.

Rodriguez-Rocha, H., Gomez-Gutierrez, J.G., Garcia-Garcia, A., Rao, X.M., Chen, L., McMasters, K.M., and Zhou, H.S. 2011. Adenoviruses induce autophagy to promote virus replication and oncolysis. *Virology* **416**, 9–15.

Sir, D., Kuo, C.-f., Tian, Y., Liu, H.M., Huang, E.J., Jung, J.U., Machida, K., and Ou, J.-h.J. 2012. Replication of hepatitis C virus RNA on autophagosomal membranes. *J. Biol. Chem.* **287**, 18036–18043.

Tanida, I., Ueno, T., and Kominami, E. 2008. LC3 and autophagy. *Methods Mol. Biol.* **445**, 77–88.

Wong, J., Zhang, J., Si, X., Gao, G., Mao, I., McManus, B.M., and Luo, H. 2008. Autophagosome supports coxsackievirus B3 replication in host cells. *J. Virol.* **82**, 9143–9153.

Xi, X., Zhang, X., Wang, B., Wang, T., Wang, J., Huang, H., Wang, J., Jin, Q., and Zhao, Z. 2013. The interplays between autophagy and apoptosis induced by enterovirus 71. *PLoS ONE* **8**, e56966.

Zhang, Y., Li, Z., Ge, X., Guo, X., and Yang, H. 2011. Autophagy promotes the replication of encephalomyocarditis virus in host cells. *Autophagy* **7**, 613–628.

Zhao, Z., Fux, B., Goodwin, M., Dunay, I.R., Strong, D., Miller, B.C., Cadwell, K., Delgado, M.A., Ponpuak, M., Green, K.G., and *et al.* 2008. Autophagosome-independent essential function for the autophagy protein Atg5 in cellular immunity to intracellular pathogens. *Cell Host Microbe* **4**, 458–469.